

Positive Tolman Length in a Lattice Gas with Three-Body Interactions

A. Tröster and K. Binder*

Johannes Gutenberg Universität Mainz, Staudingerweg 7, D-55099 Mainz, Germany

(Received 14 July 2011; published 20 December 2011)

We present a new method to determine the curvature dependence of the interface tension between coexisting phases in a finite volume from free energies obtained by Monte Carlo simulations. For the example of a lattice gas on a 3D fcc lattice with nearest neighbor three-body interactions, we demonstrate how to calculate the equimolar radius R_e as well as the radius R_s of the surface of tension and thus the Tolman length $\delta(R_s) = R_e - R_s$. Within the physically relevant range of radii, $\delta(R_s)$ shows a pronounced R_s dependence, such that the simple Tolman parametrization for the interface tension is refutable. For the present model, extrapolation of $\delta(R_s)$ to $R_s \rightarrow \infty$ by various methods clearly indicates a positive limiting value.

DOI: 10.1103/PhysRevLett.107.265701

PACS numbers: 64.60.De, 05.10.Ln, 64.60.qe, 64.75.Gh

The dependence of the interface tension σ between a metastable phase coexisting with a droplet (or bubble) of the stable phase on the radius of curvature R of the interface is of central interest for the understanding of nucleation and phase separation phenomena at first order phase transitions in fluids [1–5], a subject which is of major importance in physics, chemistry, biology and industrial applications. Curved interfaces also play an important role in the study of membranes, vesicles, and fluids in porous materials and other cavities. Since the local coordination of particles within a curved interface changes with its curvature, one expects $\sigma = \sigma(R)$, but a quantitative assessment of this dependence is difficult. Typically, R is on the nanoscale, and the interface tension differs markedly from its macroscopic limit. This problem hampers the prediction of nucleation rates from rain droplets in the atmosphere to precipitates in alloys to gas bubbles in cavitation processes, creation of foam materials, etc.

Even though it is difficult to characterize metastable states within rigorous thermodynamics of infinite systems [6], in finite systems a phenomenological analysis of the stability of interfacial states is a well-defined problem [7,8]. More than 60 years ago, Tolman [9] in a seminal paper introduced a phenomenological parametrization

$$\sigma(R) = \sigma_\infty / (1 + 2\delta/R), \quad \sigma_\infty = \sigma(R = \infty), \quad (1)$$

the length scale δ being the famous *Tolman length*. Unfortunately, it is difficult to clarify the range of radii R for which Eq. (1) holds and to predict δ within statistical mechanics (for a survey of the ongoing controversial discussion see Refs. [10–16] and the vast literature quoted therein). Applications in nucleation theory often use $\sigma(R) = \sigma_\infty$ for any R (“capillarity approximation”), but this is expected to lead to severe errors for, e.g., derived nucleation rates. Mean-field approaches such as density functional calculations [10–16] to study the validity of Eq. (1) also involve considerable approximations like neglecting capillary wave type fluctuations of the interface,

etc. A method that allows us to extract $\sigma(R)$ and δ directly from Monte Carlo (MC) or molecular dynamics data should be able to avoid all these inaccuracies, being only subject to controllable finite size effects and statistical errors.

An ideal model for studying $\sigma(R)$ in such simulations should be computationally as cheap as possible. In particular, one may resort to lattice models with short range interactions instead of off-lattice continuum models that usually spend orders of magnitude more CPU time on potential and force computations. However, in cases which may seem appealing at first glance the existence of a well-defined nonzero δ is ruled out by at least two no-go theorems. (i) One does not expect the Tolman formula (1) to hold in two-dimensional systems [17,18]. (ii) δ must vanish by symmetry for models with a symmetry relation between the microstates of the coexisting phases [19], which rules out, e.g., Ising lattice gas models built from pair interactions.

The aim of the present Letter is twofold: (i) To devise an efficient lattice model for studying Eq. (1); (ii) to develop a methodology to extract information on $\sigma(R)$ and δ from simulations.

As to point (i), consider a face-centered cubic Ising lattice in 3 dimensions with volume $L \times L \times L = V$ and periodic boundary conditions. Each of its $N = V/2$ lattice sites i is surrounded by 12 nearest neighbor sites and 24 different triangles $\langle ijk \rangle$ of mutual nearest neighbor sites. In the decade from 1970 to 1980, the triplet spin Ising fcc model with Hamiltonian

$$\mathcal{H}[\{s_i\}] = - \sum_{\langle ijk \rangle} s_i s_j s_k, \quad (2)$$

derived from this lattice topology, has been investigated for possible critical behavior (see Refs. 3–8 in Ref. [20]), until it was finally realized [20] that it actually undergoes a clearly detectable albeit weak *first order* transition. Since then, the model seems to have abruptly fallen from grace in

the literature. However, for our present purposes it is just perfect. Because of its obvious asymmetry with respect to a global spin flip we can identify its ferromagnetic ground state $\{s_i = +1\}_{i=1}^N$ of energy $-8N$ with the zero temperature “fully condensed” lattice gas phase, and the high temperature disordered phase with the “vapor.” Taking the lattice gas point of view, we parametrize the system by the number of up-spins $N_+ = \frac{1}{2} \sum_i (1 + s_i)$ rather than the magnetization, such that the corresponding density $\rho := N_+/V$ is confined to values between 0 and 0.5.

Observation of a double peak in the energy probability distribution around $T \approx 11.4$ (setting $k_B = 1$) with thermal Metropolis MC simulation based on single spin flips confirms the first order character of the transition in zero external field. By imposing equal areas under the two well-separated Gaussian-like peaks (see, e.g., [21]) and linear extrapolation of the resulting finite size phase coexistence temperatures $T_0^{(L)}$ in $1/L \rightarrow 0$ gives the estimate $T_0 = 11.39 \pm 0.01$ for the first order transition temperature of the model. However, since the first order character is not very strong, we decide not to study zero field phase coexistence right at T_0 , but work at a somewhat lower temperature $T_c = 8.0 \approx 0.7T_0$, introducing an external compensating field coupling $-H \sum_i s_i$ to reestablish symmetry in the potential minima and thereby restore conditions of phase coexistence. For each finite L , the probability distribution of N_+ now shows a double peak provided H is near the finite size coexistence value $H_c^{(L)}$, which we again define by an equal area rule. At $T = T_c$ we report the linear extrapolation $H_c^\infty \approx -3.495$ for $1/L \rightarrow 0$. Because of the dense cubic packing of fcc sites and the large coordination number we do not expect to see any noticeable anisotropy in the interface tension, which is, e.g., in the standard 3D simple cubic Ising model lower than 1% at comparable values of the reduced temperature [22].

With parameters T_c and H_c tuned for phase coexistence, we compute the dimensionless “excess” free energy density $\hat{f}(\rho) \equiv F(T_c, V\rho, H_c^\infty)/(T_c V)$ from Wang-Landau [21] simulations followed by an average over 20 independent MC production runs, considering linear system sizes $L = 18, 20, 22, \dots, 30$ (cf. Fig. 1). As expected, $\hat{f}(\rho)$ shows a pronounced asymmetry. By numerical differentiation with respect to ρ we obtain the dimensionless chemical excess potential $\hat{\mu}(\rho)$ (see Fig. 2 below). We now concentrate on the analysis of microstates containing a spherical “droplet” or cavity (“bubble”) of up-spins. Even though simulation snapshots [13,15] and comparisons of slopes of $\hat{f}(\rho)$ and $\hat{\mu}(\rho)$ [8] may give a clue about the density regions populated mainly by phase separated configurations of spherical symmetry, we avoid any prejudice in this respect by deliberately including a much larger range of possible densities in our analysis, the only requirement being that this range should safely include the spherical one. If the data are analyzed imposing spherical

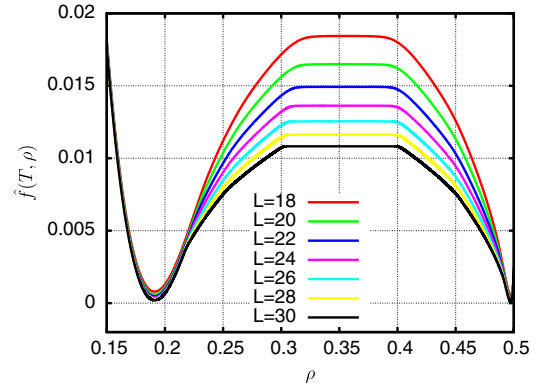


FIG. 1 (color online). Dimensionless excess free energy density \hat{f} .

symmetry in the underlying formulas, deviations from the expected behavior allow us to locate the spherical density domains *a posteriori*. For a given total density ρ of an inhomogeneous phase separated state with dimensionless grand potential density $\hat{\omega}(\hat{\mu}) = f(\rho) - \hat{\mu}\rho$, the equation $\hat{\mu}(\rho_i) \equiv \hat{\mu} = \hat{\mu}(\rho)$ generally has two additional solutions $\rho_i, i = \alpha, \beta$ representing the homogeneous densities of the coexisting condensed and disordered phases with $\hat{\omega}_i(\hat{\mu}) = f(\rho_i) - \hat{\mu}\rho_i, i = \alpha, \beta$. We impose a spherical dividing surface $A(R)$ of radius R , which splits the total volume into $V = V_\alpha(R) + V_\beta(R)$, and assume the smaller one to be spherical with radius R . This gives rise to an excess grand potential density

$$\Omega^x(R; \hat{\mu}) = V\hat{\omega}_i(\hat{\mu}) - V_\alpha(R)\hat{\omega}_\alpha(\hat{\mu}) - V_\beta(R)\hat{\omega}_\beta(\hat{\mu}), \quad (3)$$

from which we obtain the R -dependent dimensionless interface tension

$$\sigma(R) = \Omega^x(R; \hat{\mu})/A(R). \quad (4)$$

The dimensionless interface tension $\sigma_s \equiv \sigma(R_s)$ at the radius R_s of the so-called *surface of tension* is found numerically by locating the minimum of $\sigma(R)$ with respect to R in accordance with the universal $d = 3$ formula [23] $\sigma(R)/\sigma(R_s) = 1 + (1/3)(1 - R_s/R)^2(1 + 2R/R_s)$. The equimolar interface tension $\sigma_e \equiv \sigma(R_e)$ at the equimolar radius R_e is determined by the lever rule

$$\frac{V_\alpha(R_e)}{V} = \frac{\rho_\beta - \rho}{\rho_\beta - \rho_\alpha}, \quad \frac{V_\beta(R_e)}{V} = \frac{\rho - \rho_\alpha}{\rho_\beta - \rho_\alpha}. \quad (5)$$

The difference $\delta(R_s) := R_e - R_s$ is the famous Tolman length. The simple Tolman formula (1) can be derived [23,24] only under the crucial assumption of *constant* δ . To detect a nontrivial R_s -dependence of δ , we assemble our resulting data for $\delta(R_s)$ (droplets) and $-\delta(R_s)$ (bubbles) in Fig. 3. And indeed, $\delta(R_s)$ appears to be far from constant in the observed range of radii. Plotted against $1/R_s$, Fig. 3 shows three ranges of different characteristics. In particular, roughly in the interval of inverse radii between 0.1 and 0.2 we notice a certain tendency of the

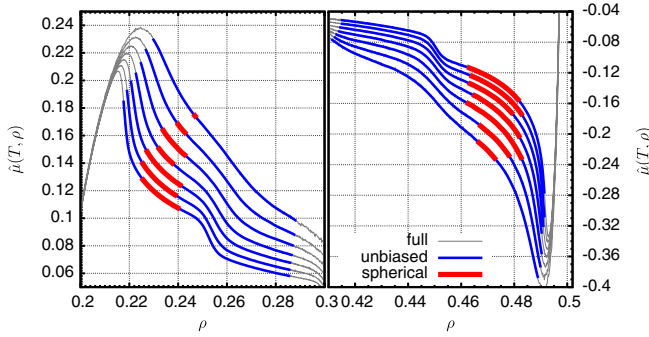


FIG. 2 (color online). Full excess chemical potential $\hat{\mu}(\rho)$ with indicated unbiased density ranges initially used in our analysis and actual spherical density ranges as determined by localizing the linear sections of $\delta(R_s)$ as functions of $1/R_s$.

data to populate a common “master curve” with linear slope, such that for large L a convergence towards an L -independent function $\delta(R_s)$ takes place for both droplets and bubbles. Quantitatively, the corresponding radial ranges can be pinned down by determining the start and end points where a linear fit to $\delta(R_s)$ starts to break down by visual inspection (Fig. 4). Interestingly, as shown in Fig. 2, the corresponding total density ranges calculated from these radii are in excellent correspondence with those densities for which one may indeed observe spherical droplets and bubbles as the abundant microscopic configurations in simulation snapshots. Consistency checks of the spherical density and radial ranges determined by the above procedure are provided by monitoring various observables computed under presupposed spherical symmetry. As an example, Fig. 5 shows the excess free energy $F_e^x = V f_e^x$ at R_e as a function of $\hat{\mu}$. Again we see that the common part where all curves collapse onto a “master curve” yields well-defined functions $F_e^x(\hat{\mu})$ for both bubbles and droplets. Isolating these deviations from the spherical regime would have been difficult based exclusively on interface tension data (Fig. 6). Interestingly, these data reveal a striking “overshooting” of the bubble data for $1/R_s \rightarrow 0$, and applying formula (1) would hint at a

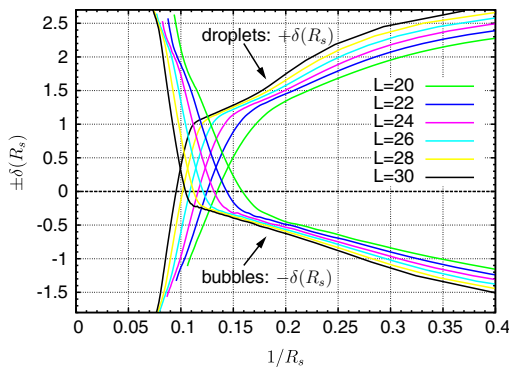


FIG. 3 (color online). Raw data for Tolman length $\delta(R_s)$ computed under the assumption of spherical interface geometry.

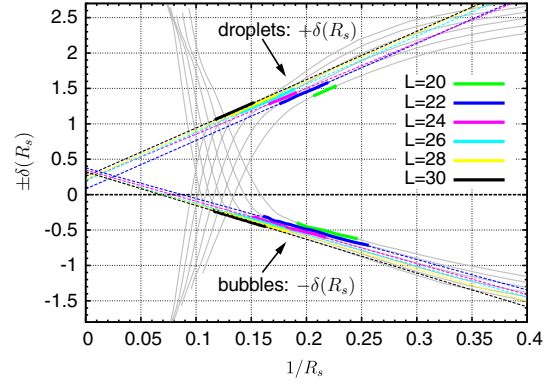


FIG. 4 (color online). Extrapolation of linear sections of $\delta(R_s)$ as functions of $1/R_s$ [(+): droplets, (-): bubbles]. Gray curves correspond to unbiased density ranges, their colored sections, and linear extrapolations to the spherical regime (cf. Fig. 2).

positive limit $\delta > 0$ for droplets. However, such conclusions are premature; as emphasized above, $\delta(R_s)$ is not constant and the use of (1) is questionable. Rather, an extrapolation of the straight sections for $\delta(R_s)$ in Fig. 4 to $R_s \rightarrow \infty$ is needed, i.e., monitoring the intersection points of the corresponding fitted lines with the axis $1/R_s = 0$. And indeed, Fig. 4 clearly reveals a tendency of these intersection points to converge towards a positive limit $\delta := \lim_{R_s \rightarrow \infty} \delta(R_s)$ estimated as $\delta \approx 0.3$.

To back up this observation, we have also tested alternative ways to obtain the limiting value δ from our data. In $d = 3$, $\delta(R_s)$ is related to the adsorption $\Gamma_s = \Gamma(R_s)$ at the surface of tension by the exact cubic equation [25]

$$\frac{\Gamma_s}{\Delta\rho} = \delta(R_s) \left[1 + \frac{\delta(R_s)}{R_s} + \frac{1}{3} \left(\frac{\delta(R_s)}{R_s} \right)^2 \right], \quad (6)$$

where $\Delta\rho = \rho_\alpha - \rho_\beta$ denotes the density difference of both coexisting phases. In Γ_s , we also observe linear sections in $1/R_s$ which allow extrapolation to $R_s \rightarrow \infty$ (not shown). Together with the limiting planar interface

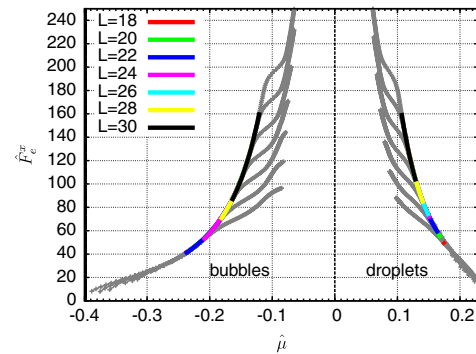


FIG. 5 (color online). Equimolar excess free energy $F_e^x(\hat{\mu})$ as function of $\hat{\mu}$. Gray curves correspond to unbiased density ranges, their colored sections to the spherical regime (cf. Fig. 2).

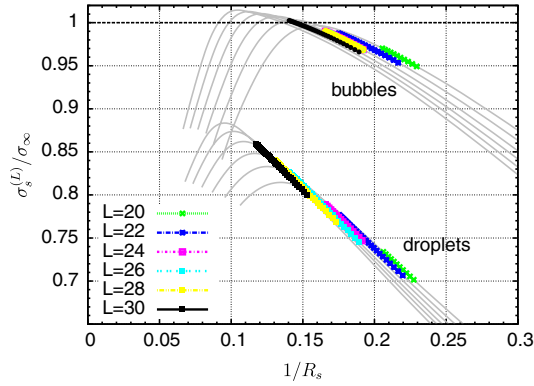


FIG. 6 (color online). Reduced finite size interface tensions $\sigma_s^{(L)}/\sigma_\infty$ at R_s , (σ_∞ denotes the planar interface tension). Gray curves correspond to unbiased density ranges, their colored sections to the spherical regime (cf. Fig. 2).

value $|\Delta\rho_\infty| = 0.3055 \pm 0.0001$, these data confirm the trends observed in Fig. 4. In the spherical regime, there is a one-to-one correspondence $R_s = R_s(\hat{\mu})$ with $R_s \rightarrow \infty$ for $\hat{\mu} \rightarrow 0$ and vice versa. Investigating the limiting behavior of $\delta[R_s(\hat{\mu})] \equiv \delta(\hat{\mu})$ for $\hat{\mu} \rightarrow 0$, a linear relation between $\delta(\hat{\mu})$ and $\hat{\mu}$ has recently been reported in [26], which is quite reminiscent of our present approach. Indeed, upon performing the above reparametrization we also observe a roughly linear behavior in the spherical data regime. Fitting straight lines to these sections once again produces another set of extrapolated limiting values for δ with similar visual appearance and convergence tendencies as the ones we obtained using our previous methods. All our attempts to extrapolate $\delta(R_s)$ to $R_s \rightarrow \infty$ indicate a nonzero limiting value, which we roughly estimate as $\delta \approx 0.33$ (cf. Fig. 7).

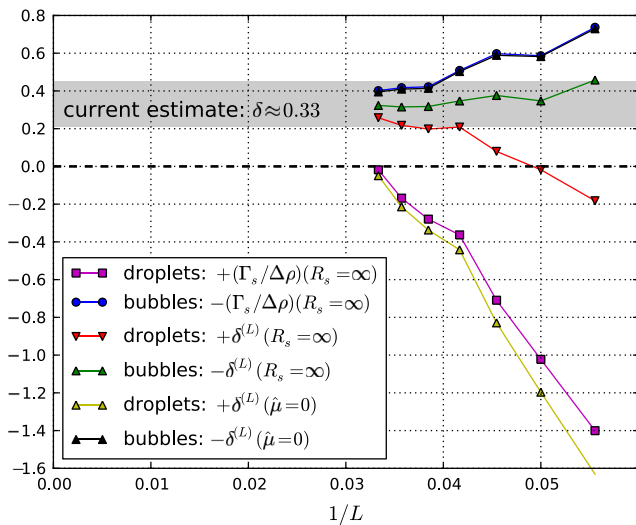


FIG. 7 (color online). Summary of Tolman length $\delta = \lim_{R_s \rightarrow \infty} \delta(R_s)$ estimates obtained from the different methods discussed.

Summarizing, we have presented several related approaches to extract the Tolman length $\delta(R_s)$ of a three-spin interacting Ising lattice gas on an fcc lattice from free energies obtained by MC simulations. Within the considered system sizes, $\delta(R_s)$ shows a strong dependence on R_s . Unlike in the vapor-to-liquid transition of Lennard-Jones fluids, where the limiting value $\delta = \lim_{R_s \rightarrow \infty} \delta(R_s)$ seems to be slightly negative, for the present model we observe a clear tendency of $\delta(R_s)$ to saturate at a positive limit $\delta > 0$. To demonstrate this in a completely stringent way and give a numerically reliable estimate would require going to *much* larger system sizes. However, as will be shown for a Lennard-Jones fluid in a forthcoming paper, this extrapolation is rather academic, at least as far as nucleation theory is concerned. In fact, one can show that at the radii for which $\delta(R_s)$ has saturated sufficiently, the corresponding nucleation barriers already exceed some $100k_B T_c$ or more (cf. also Fig. 6). Thus, neither the capillarity approximation nor the Tolman parametrization Eq. (1) should be employed in any serious quantitative work. In contrast, results such as those shown in Figs. 5 and 6 yield precisely the information needed in predicting nucleation rates. Of course, further work will be needed to generalize our approach to more specific models of materials.

A. T. acknowledges support by the Austrian Science Fund (FWF) under Project No. P22087-N16.

*troestea@uni-mainz.de

- [1] D. W. Oxtoby, *J. Phys. Condens. Matter* **4**, 7627 (1992).
- [2] J. L. Katz, *Pure Appl. Chem.* **64**, 1661 (1992).
- [3] P. G. Debenedetti, *Metastable Liquids* (Princeton University Press, Princeton, New Jersey, 1996).
- [4] D. Kashchiev, *Nucleation: Basic Theory with Applications* (Butterworth Heinemann, Oxford, UK, 2000).
- [5] M. P. Anisimov, *Russian chemical reviews* **72**, 591 (2003).
- [6] O. Penrose and J. Lebowitz, *J. Stat. Phys.* **3**, 211 (1971).
- [7] K. Binder and M. H. Kalos, *J. Stat. Phys.* **22**, 363 (1980).
- [8] K. Binder, *Physica A (Amsterdam)* **319**, 99 (2003).
- [9] R. C. Tolman, *J. Chem. Phys.* **17**, 333 (1949).
- [10] J. C. Barrett, *J. Chem. Phys.* **124**, 144705 (2006).
- [11] M. A. Anisimov, *Phys. Rev. Lett.* **98**, 035702 (2007).
- [12] A. E. van Giessen and E. M. Blokhuis, *J. Chem. Phys.* **131**, 164705 (2009).
- [13] M. Schrader, P. Virnau, and K. Binder, *Phys. Rev. E* **79**, 061104 (2009).
- [14] J. G. Sampayo *et al.*, *J. Chem. Phys.* **132**, 141101 (2010).
- [15] B. J. Block *et al.*, *J. Chem. Phys.* **133**, 154702 (2010).
- [16] Y.-Q. Xue *et al.*, *J. Phys. Chem. B* **115**, 109 (2011).
- [17] J. R. Henderson and J. S. Rowlinson, *J. Phys. Chem.* **88**, 6484 (1984).
- [18] M. J. P. Nijmeijer *et al.*, *J. Chem. Phys.* **96**, 565 (1992).

- [19] M. P. A. Fisher and M. Wortis, *Phys. Rev. B* **29**, 6252 (1984).
- [20] O. G. Mouritsen, S. J. Knak Jensen, and B. Frank, *Phys. Rev. B* **23**, 976 (1981).
- [21] D. Landau and K. Binder, *A Guide to Monte Carlo Simulations in Statistical Physics* (Cambridge University Press, Cambridge, 2009), 3rd ed..
- [22] E. Bittner *et al.*, *Nucl. Phys.* **B820**, 694 (2009).
- [23] J. Rowlinson and B. Widom, *Molecular Theory of Capillarity* (Dover Pub., Inc., Mineola, NY, 1982).
- [24] S. Ono and S. Kondo, in *Handbuch der Physik*, edited by S. Flügge (Springer, Berlin, 1960), Vol. 10, p. 134.
- [25] K. Koga *et al.*, *J. Chem. Phys.* **109**, 4063 (1998).
- [26] J. Julin *et al.*, *J. Chem. Phys.* **133**, 044704 (2010).